*Sensors & Transducers, Vol. 22, Special Issue, June 2013, pp. 147-154*

**Sensors & Transducers**

*http://www.sensorsportal.com*

# Develop a Framework of Ferro-Magnetization Sensor on Weightlessness in Modified Bessel Analysis

**Je-Ee Ho**
Department of Mechanical Engineering, National Ilan University,
No. 1, Sec. 1, Shennong Rd., Yilan City, Yilan County 260, Taiwan (R.O.C.)
Tel.: +886939838749
E-mail: jeho@niu.edu.tw

*Received: 15 April 2013 /Accepted: 20 June 2013 /Published: 28 June 2013*

**Abstract:** A framework of ferro-magnetization on apparent weightiness, through electro-magnetic induction, is proposed in this study. Here the integral solution of ferro-magnetization, based on Boltzmann probabilistic theory in modified Bessel function, avoids unstable result accessed from traditional Langevin's analysis. Also, a self-designed electromagnetism mechanism measuring gravitational counteraction of testing sample is set up and used to evaluate its magnetic behavior on apparent weight. That not only features as a simple device with economical cost and easy operation, but also could be further extended to the application of ferro-magnetization sensor. While compared to the results measured from Vibration Sample Magnetometer (VSM) for ferro-product provided by Matsumoto co., magnetization curve of self-prepared ferro-sample, base on present measuring method, shows an excellent agreement within the working region of 0~36 mT , in which the maximum relative error 100 %, evaluated from traditional classic Langevin theorem, could be remarkably reduced to 20 %.


**Keywords:** Gravitational counteraction, Ferro-magnetization.

## 1. Introduction

Formerly the classic Langevin theory, with the assumption of colloidal magnetic particles embedded in saturation moment, was widely used to determine the super-paramagnetic behavior of ferro-fluid [1]. Indeed, the ferro-particles are randomly oriented and initially have no net magnetization. Under the presence of magnetic intensity, the produced dipole moment will turn around ferro- particles to field direction as shown in Fig. 1, and the aligning tendency will continuously increase until the saturation magnetization is reached. Hence the over-estimation based on the classic model seems to be not so surprised. To understand the magnetization of ferro-fluid vs. the field intensity, a DC electromagnetic experimental device was set up and conducted in a rotary shaft to examine the magnetic behavior of ferro-fluid [2, 3]. Unfortunately, the rise of working temperature, during working process, seems to be inevitable and usually results in the variation of viscosity to make analytic procedure more complicated. Another micro/nanoscale pumping device with AC magnetic field was also considered to survey the magnetization of ferro-fluid [4, 5]. Whether the fluid moves opposite to the direction of field (backward pumping) or in the same direction of field (forward pumping) primarily depends on the frequency of AC power supplied, which usually gives rise to another trouble problem " so called magnetization lag". Generalized from previous ferrohydrodynamical application, several additional apparatus should be calibrated to guarantee the stability of magnetic behavior. That not only makes a tedious experimental procedure but also significantly increases the expense of experiment [6]. Recently, an advanced measuring technology with Vibration Sample Magnetometer (VSM) has been developed to characterize the magnetization of nanoparticles [7, 8]. By this way, relevant magnetic characteristic including effective dipole moment, agglomeration of colloidal particles and orientation of magnetic particles, could be exactly captured and transferred to PC directly. Although the measurement made by VSM has shown its special advantage over conventional measuring methods, the charge for relevant equipment is usually too expensive to be affordable for local laboratory.

To improve above insufficient, a fundamental working principle of sensor related to ferro-magnetization on ferro-weightlessness draws our attention in this study. Here an economical DC electromagnetic system with easy operation will be self-designed to magnetize the ferro-sample. Coupling the action of ferro-magnetization and field intensity, an upward magnetic pressure will be induced to counteract the gravity effect and which reduces the apparent weight of ferro-sample. While invoking the balance of weight loss and electromagnetic force, ferro-magnetization could be successfully carried out by iterating Bessel function implicitly. In addition, the discussion of chemical precipitation to prepare ferro- sample will be also included in this study.

## 2. Analysis

Prior to formulate the modified Bessel function of ferro-magnetization on apparent weight loss, several reasonable assumptions without losing the overall behavior should be made in advance.

### 2.1. Assumptions

1. Compared with external magnetic strength, Van der Waals force between the interactions of colloidal particles is small enough and can be neglected.
2. Magnetic field induced in the middle region of long solenoid is assumed to be uniform.
3. By the definition of volumetric fraction Φ for ferro-particles in reference [1], a linear relation $M=\Phi M_S$ will be taken into account, where the symbols of $M$ and $Ms$ indicate ferro-magnetization of ferro-fluid and magnetic particle respectively.

### 2.2. Governing Equations

While we start analysis process, ferro-particles in spatial distribution should be introduced first. Initially, ferro-particles in a colloidal solution are randomly oriented. However, the changing situation will emerge as dipole moment begins to turn around to align with ordinary field (see Fig. 1) and the tendency will becomes visible if the magnitude of field is increased. In other words, further intensify ferro-magnetization will produce strong body torque to rotate ferro- particles to field direction. Indeed, magnetic attraction is primarily dependent on the magnetization degree and field intensity and which will counteract the ferro-gravity and reduces the weight of ferro-sample promptly provided that an upward field direction is set.

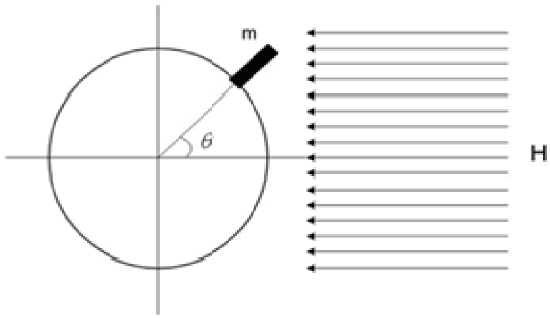


**Fig. 1.** Orientation configuration of ferro-particles along field direction.

Next we will proceed to treat with magnetic behavior of ferro-sample, here both basic formulas, dealing with field average magnetization and magnetic induction, will be yielded in Eqs.(1) and (2) respectively.

$$\overline{M} = \frac{1}{H}\int_0^H MdH = \chi M \quad , \tag{1}$$

$$B = \mu_0 H \quad , \tag{2}$$

where the value of $\chi = \overline{M}/M$ is estimated to be 0.5~1, $\overline{M}$ & $M$ being the field-average magnetization and instant magnetization of ferro-fluid respectively, and $B$ is defined as the magnetic flux intensity.

To distinct the physical meaning of instant magnetization $M$ and field-average magnetization $\overline{M}$, a clear interpretation will be given below. In Fig. 2, the shaded area, under magnetization profile, relates to magnetic pressure induced by coupling effect of ferro- magnetization $M$ and field strength $H$. Therefore field-average magnetization $\overline{M}$ could be successfully evaluated by estimating equivalent rectangular area bounded by field intensity and field-average magnetization.

Combining equations (1) and (2) gives the magnetic pressure $P_m$ in equation (3). Additionally, the gravitational counteraction of magnetic fluid, subjected to the field employed, can be expressed in equation (4)

$$P_m = \mu_0 \overline{M} H = \chi M B \ , \tag{3}$$

$$\Delta W = \int p_m dA \cos\theta = \chi \langle M \rangle BA \ , \tag{4}$$

where $A$ is the real contacted area of ferro-particles lying on the cylindrical surface, symbol $<M>$ appearing in Eq. (4) demonstrates average magnetization of magnetic fluid along field direction, and θ, in Fig. 1, is defined as oriented angle of ferro-particle measured from field direction.

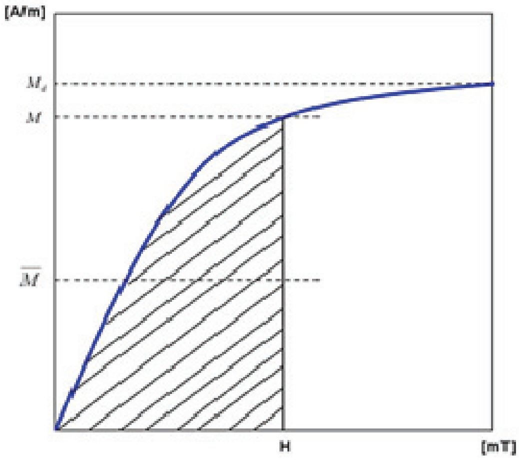


**Fig. 2.** Magnetization curve of ferro-fluid.

By appealing to the integral of Boltzmann probabilistic distribution, the ratio of $<M>/M$ of integrated form, in modified Bessel function, might be carried out in Eq. (5) and Eq. (6). In which, the values of $I_o$ and $I_1$ will approach to unity and zero respectively as a small α is considered, i.e. continuous ferro-magnetization in a weaker field could be expected.

$$\frac{\langle M \rangle}{M} = \frac{\int_0^{\pi} e^{\frac{mH}{KT}\cos\theta} \cos\theta \, d\theta}{\int_0^{\pi} e^{\frac{mH}{KT}\cos\theta} \, d\theta} = I_1(\alpha)/I_0(\alpha) \ , \tag{5}$$

$$I_n(\alpha) = \frac{1}{\pi} \int_0^{\pi} e^{\alpha \cos\theta} \cos(n\theta) \, d\theta \ , \tag{6}$$

where $K$ is the Plank's constant, $V$ is the volume of ferro-particle and

$$\alpha = \frac{mH}{KT} = \frac{M_S BV}{KT} \ ,$$

Coupling Eqs. (4) ~ (6) with assumption 3, the implicit dependence of apparent weight loss $\Delta w$ on instant magnetization of ferro-particle $M_S$ could be derived as in Eq. (7), which constitutes the main theorem of ferro-magnetization sensor in modified Bessel function. Besides, angular density of magnetic particles σ under field induction also arise our attention. In Eqs. (8), N is defined as half amount of magnetic particles deposited on the cylindrical surface, and angular density σ could be successfully developed using a mathematical model of Boltzmann probability

$$\Delta W = \chi \phi M_S BA \frac{I_1(\alpha)}{I_0(\alpha)} , \tag{7}$$

$$\sigma = \frac{N \ e^{\frac{mH}{KT}\cos\theta}}{\pi \ I_0\left(\frac{mH}{KT}\right)} = \frac{N \ e^{\alpha \cos\theta}}{\pi \ I_0(\alpha)} \ , \tag{8}$$

Unlike the continuous magnetization mentioned above, traditional Langevin's theory, in Eqs. (9), to predict ferro-magnetization should be dealt with. In which, saturated magnetization, $M_d$, assumed to be embedded in ferro-particle seems to overestimate the magnitude of $M$. Additionally, the appearance of hyper-cotangent in Eqs. (9) easily leads to an unstable iteration especially in the region of small α, in other words, a divergent calculation will be experienced for micro-study. Thus above conventional model determining the practical magnetization will be not considered in this study.

$$\frac{M}{\phi M_d} = \coth \alpha - \frac{1}{\alpha} \equiv L(\alpha) \ , \tag{9}$$

## 3. Experimental Procedure

### 3.1. Preparation of Testing Ferro-sample

Chemical precipitation, in this study, is employed to prepare the working ferro-sample, where soluble iron salts, $FeCl_3$ $6H_2$ O, $FeCl_2$ $4H_2$ O & NaOH, are fed as the reactants. Subsequently, the involvement of ammonium hydroxide leads to the agglomeration of magnetite in co-precipitation process. That allows ferro-particles separated from liquid phase in the filtration step followed. Successively chemical surfactant, after sucking water out, will be included to reduce the size of ferro-particles into a small-colloidal range, and further agglomeration will be avoided by two- hour stirring process while working temperature maintains 65~70 °C. Thus the water-based product could be developed. Next, additional steps will be required to produce oil-based product. To transform the ferro-particles from organic phase into aqueous phase, dissolving water-based product in a dispersing agent is desired. Here, continuous stirring is still undergone until the addition of methanol is fully mixed. While the mixture reaches at steady equilibrium, filtration procedure will be performed by extracting methanol out. Thus oil-based product, after adding a small amount of diesel oil, will be attained and volumetric ration occupied by magnetite determines the ferro-concentration of solution. So far, overall preparation process might be accomplished and relevant flow chart is illustrated in Fig. 3. To assess the magnetized performance of self-prepared sample, a strong magnetic attraction as magnetism approaching is induced in Fig. 4, which also weighs magnetized quality. Besides, instability of ferro-surface in Fig. 5 "so called Rosensweig phenomena " will be also accessed by refining test sample with surfactant in slow heating process .

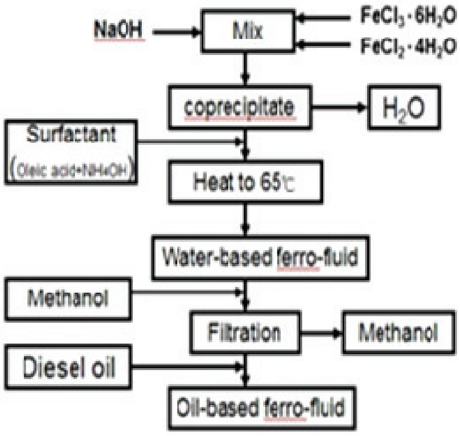


**Fig. 3.** Flow chart of preparing ferro-sample.

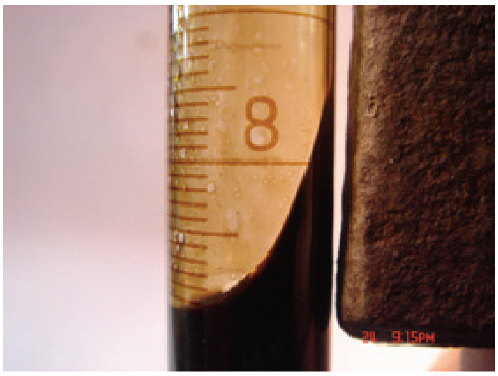

**Fig. 4.** Photography of self-preparation ferro-sample.

### 3.2. Experimental Mechanism

To examine the validity of present model, an auxiliary experimental mechanism of small size, simple structure and easy operation is depicted in Figs. 6~7. In which, several relevant components, such as working solenoid, digital measuring device as well as DC power supply, will be also included in Fig. 8~Fig. 11.

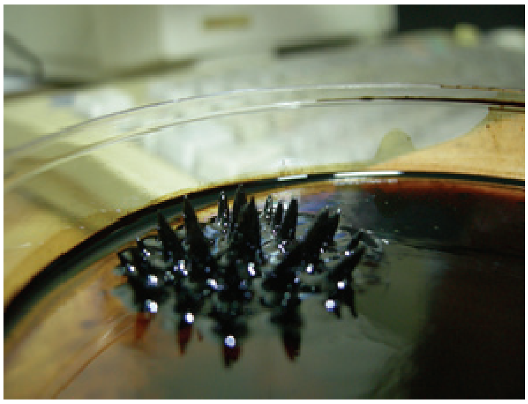

**Fig. 5.** Photography of Rosensweig ferro-instability.

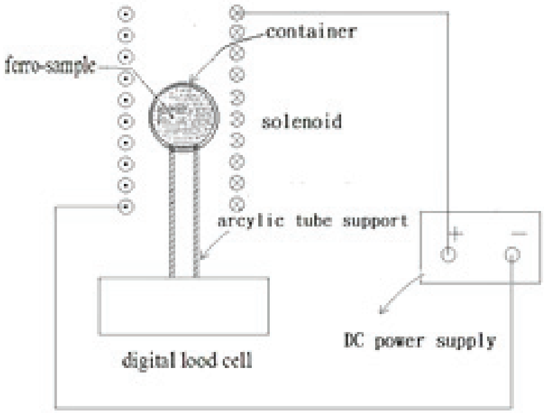


**Fig. 6.** Sketch of the experimental system.

**Fig. 7.** Photography of experimental device.

View from Fig. 8, the photography demonstrates a working solenoid, 2800 coils wound together closely, to produce working magnetic field 0~40 mT as the external voltage 0~25 V is regulated by turns.

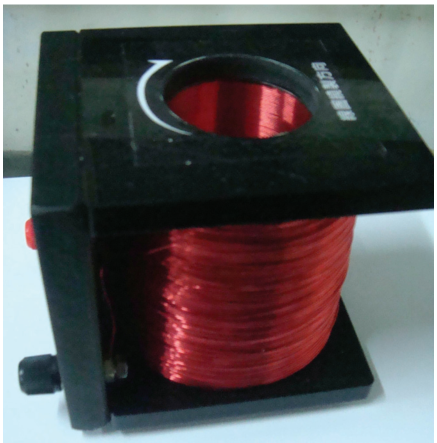

**Fig. 8.** Photography of current –carry solenoid.

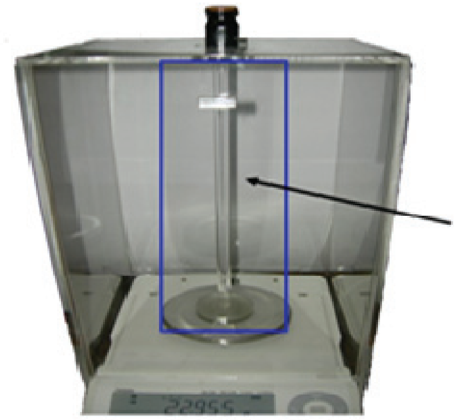

**Fig. 9.** Photography of separation acrylic tube.

To prevent the influence of magnetic field, induced by current-carry solenoid, on load cell, a long acrylic tube with dimensions of 2 cm diameter and 30 cm length, shown in Fig. 8, should be considered to separate testing sample and digital weight-meter. Below which, a measuring unit of digital load cell with resolution 0.001g,in Fig. 9, is utilized to record and display the total weight of ferro-sample and cylindrical container subjected to field enforcement. Through it, real measured data could be captured and transferred to PC promptly. Also, a DC power supply, in Fig. 10, with facility of 0~5 A and 0~30 V is used as a driving source which is able to be controlled precisely to meet the demand of working condition.

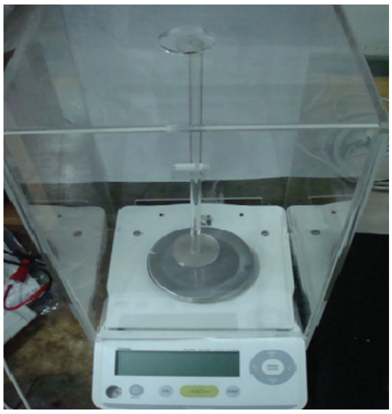

**Fig. 10.** Photography of digital load cell.

**Fig. 11.** Photography of digital load cell.

### 3.3. Experimental Procedure

Before embarking on the measuring process at working temperature 25 °C, several testing procedures are scheduled as follow.

1. Initially, read the weight of cylindrical container in the absence of ferro-sample.
2. Measure coaxial magnetic intensity inside the solenoid by regulating DC voltage 2 V ~ 30 V.
3. Place the ferro-sample in cylindrical container illustrated in Fig. 1 and record individual total weight corresponding to working DC voltage set in step 2.
4. Calculate individual weight loss by estimating the weight difference between step 3 and step 1 for each input voltage applied.
5. Assign an initial guessed value of $\chi$ and evaluate the magnetization *Ms* of ferro-particle from equation (7) using iteration method. And then calculate $\overline{M}$, $\chi$ with Simpson rule and integral skill from equation (1).Check whether the relative error of calculated and assigned $\chi$ is less than 5 %. If not, step 5 should be repeated until the convergence is accessed.
6. Steps (1)~(6) are recurred with ferro-sample of volumetric concentration 0.004 or the temperature of ferro-sample rose to 45 °C.

## 4. Results and Discussion

While investigate the induced magnetic behavior of sample for both volumetric concentrations at different working temperature, the variation of weight loss vs. magnetic flux density and calculated magnetization vs. magnetic flux density will be plotted in Fig. 12 and Fig. 13 respectively. In which, a rapid growth of weight loss, in Fig. 10, is visible within field intensity 6-18 mT and that just corresponds to a fast magnetization in Fig. 13. Moreover, the distribution in Fig. 13 also tells that saturation magnetization, 7000 A/m, predicted for concentration φ=0.04 is about ten times the value, 650 A/m, accessed from concentration φ=0.004, i.e. ferro-magnetization might be believed to be proportional to the volumetric concentration of particles. In addition, a smaller magnetization rate is found at 45 °C than that evaluated at 20 °C, and magnetized result will be further considerably decreased as in the case of φ 0.004.

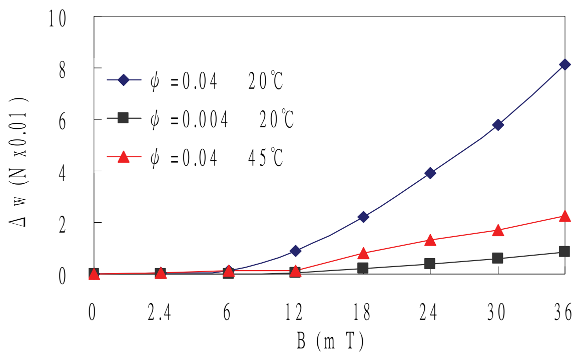


**Fig. 12.** Comparison of weight loss .vs. induced magnetic field for ϕ=0.04 (20 °C, 45 °C) and ϕ=0.004 (20 °C).

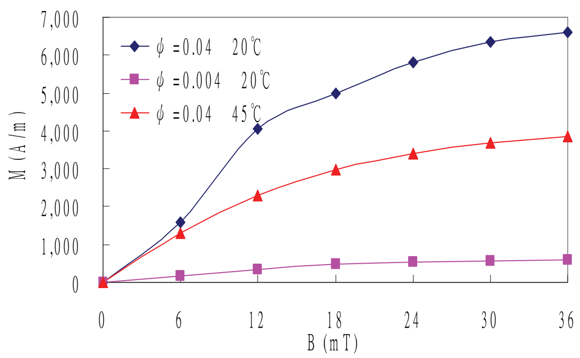


**Fig. 13.** Magnetization .vs. induced magnetic field for ϕ=0.04 (20 °C, 45 °C) and ϕ=0.004 (20 °C).

Another outcome comparison from VSM measurement, classic Langevin solution, in variable $M_d$, and Bessel theory, in variable $Ms$, is discussed in Fig. 14.

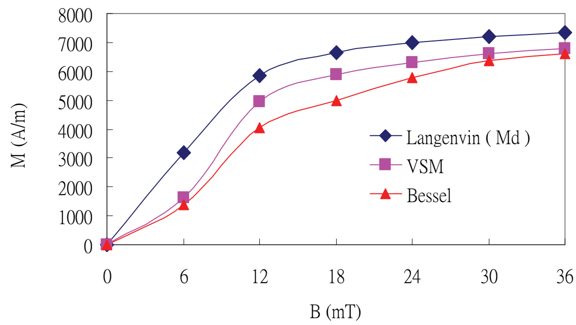


**Fig. 14.** Comparison with magnetization curves estimated from Langevin function, Bessel theory and VSM method.

From which, all the distributions, with saturation magnetization approaching to 7000 A/m, behave quite alike in high magnetic region. However, about 100 % relative error, estimated from Langevin theory, significantly deviates from the results made from VSM as magnetic intensity is less than 6 mT. That attributed to the term of hyper cotangent function in classic Langevin function easily leads to a divergent calculation during the lower field region. However, such unstable disadvantage might be overcome by the continuity of Bessel theory using successive implicit iteration. As a result, the maximum relative error, occurring at lower magnetic field, could be effectively dropped down to 20 %.

Until now, our discussion was focused on the survey of induced magnetic behavior. Subsequently we will proceed to discuss the angular distribution of magnetic particles under the presence of magnetic field. It might also predict real contacted area of ferro-particles depositing along the cylindrical surface. To estimate the area $A$, a physical meaning is introduced as follows. Initially, ferro- particles are assumed to be uniformly distributed along inner semi-cylindrical surface as the absence of field. As magnetic field becomes active, ferro- particles will move forward to align with the field due to the action of magnetic attraction, and that makes the initial orientation of ferro-particle re-distributed. Consequently, the angular density in the rear region of inner semi-cylinder surface becomes much weaker than initial value, and such rear region will be excluded from the contacted area considered. Thus contacted area $A$ for various magnetic strength applied could be predicted by the intersected point of horizontal dotted line (initial magnetic field is absent) and individual angular distribution curve drawn in Fig. 15. While compared with individual angular density at θ= 0° (see Fig. 1) for concentration ratio ψ=0.04 at working temperature 20 °C, Fig. 15 reveals that initial angular density σ is about 0.33 $N/m^2$ (as the indication of dotted line), and the value will quickly increase to 2.5 $N/m^2$ if magnetic strength increases to 36 mT. That means more and more magnetic particles will be attracted gather to the front region of cylinder surface and the effective contacted area lessening from angle θ= 60° to θ= 45° will be accessed as the magnetic intensity varies from 6 mT to 36 mT. In addition, the area under individual curve also sates half amount of magnetic particles N lying along the semi- cylindrical surface, and this area, after deliberate calculation, is found to be nearly the same for different cases Hence the distribution of σ obeying mass conservation law could be confirmed.

Finally, our discussion will be turned to determine field-average magnetization coefficient χ. In order to evaluate the value, Eqs. (1) together with modified Bessel Eqs. (7) constitutes an implicit loop, in which the continuous iteration by Simpson rule & trial and error method will go through. Consequently, the value of χ about 0.5 for ψ=0.04 and 0.004 is kept under magnetic intensity less than 12 mT applied i.e.

both nearly horizontal lines will be resulted in Fig. 16. After then, field-average coefficient exhibits a slow increase from 0.5~0.68 as magnetic flux is extended to 36 mT. On the whole, calculated results from above ferro-concentration are found to be consistent and which might be also identified from the distribution of magnetization curves in Fig. 14.

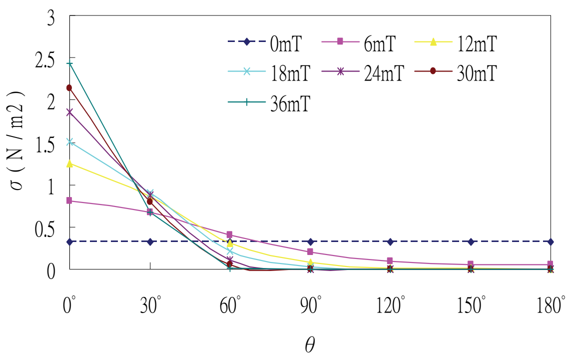


**Fig. 15.** Ferro-particles in angular distribution .vs. magnetic intensity applied for ϕ=0.04 at working temperature 20 °C.

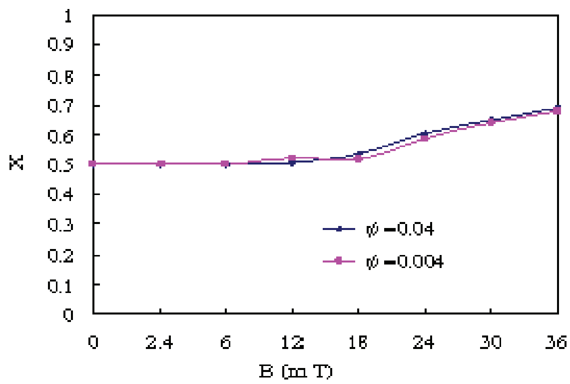


**Fig. 16.** Field-average magnetization coefficient .vs. magnetic intensity applied for ϕ=0.04 and ϕ=0.004 at working temperature 20 °C.

## 5. Conclusions

Summary from above discussion, the validity of working principle for ferro-magnetization sensor on apparent weight could be identified. Here magnetization curve predicted by classic Langevin function is apparently overestimated and seems to be only applicable in the case of ferro-particle embedded with saturation magnetization. However, our proposed model, practical ferro-magnetization depending on field applied, has the special advantage toward the exact magnetic behavior. Also, the unstable divergence resulting from classic Langevin model can be fully avoided by using modified Bessel function of zero and first kind as in the case of smaller magnetic intensity. When investigate the measured results, a fast growth of weight loss will be initiated as the rapid magnetization of ferro-particle starts working, and then a linear profile with slow growth will be followed until saturated magnetization is achieved. In addition, magnetic performance of testing sample is also found to be proportional to volumetric fraction of solid particles, and a reversed effect disturbing the consistence of suspended particles will occur as the ferro-sample in higher working temperature. Therefore it is believed that the alignment of particles to the field direction will be further interrupted by thermal agitation and this will cause a magnetization lag as well.

## 6. Nomenclature

| | |
|---|---|
| $A$ | Real contacted area of the particles along the cylindrical surface [m$^2$] |
| $B$ | Magnetic flux [mT] |
| $H$ | Magnetic intensity [A /m] |
| $K$ | Boltzmann constant |
| $M$ | Magnetization of ferro-fluid [A /m] |
| $N$ | Half amount of ferro-particles |
| $\Delta W$ | Apparent weightlessness of ferro-fluid [ kg] |
| $M_d$ | Saturation magnetization of ferro-particle [A |
| $M_s$ | Practical magnetization of ferro-particle [A |
| $\overline{M}$ | Mean magnetization of ferro-fluid [A /m] |
| $P_m$ | Induced magnetic pressure [Pa] |
| $T$ | Temperature of ferro-fluid [K] |
| $V$ | Volume of ferro-particle [m$^3$] |
| $m$ | Dipole moment of ferro-particle |
| σ | Angular density of magnetic particles |
| $\theta$ | Position angle of particles to field direction |
| χ | field-average magnetization coefficient |
| ψ | Volumetric concentration of ferrousample |
| $\mu_0$ | Permeability of free space [Henery /m] |

## References


[1]. R. E. Rosensweig, Ferrohydrodynamics, *Cambridge University Academic Press,* London, 1986.

[2]. R. E, Rosensweig, Negative viscosity in a magnetic fluid, L. Marton, Ed., *Academic Press*, New York, Vol. 48, 1996, pp. 103-99.

[3]. M. Zhan, Magnetic fluid and nanoparticle applications to nanotechnology, *Journal of Nanoparticle Research*, 3, 2001, pp. 73-78.

[4]. Zahn and D. R. Greer, Ferrohydrodynamic pumping in spatially uniform sinusoid ally time-varying magnetic fields, *J. Magnet. Mag. Mat.,* 149, 1995, pp. 165-173.

[5]. M. Zahn and D. R. Greer, Ferrohydrodynamic pumping in spatially uniform sinusoid ally time-varying magnetic fields, *J. Magnet. Mag. Mat.,* 149, 1995, pp. 165-173, 24-38.

[6]. Nicole Pamme, Magnetism and microfluidics, *Lab Chip*, 6, 2006.

[7]. Je-Ee Ho, Measuring the Magnetization of Nano Ferro-fluid with D. C Electromagnetic Application,

*International Journal of Applied Science and Engineering,* Vol. 6, No. 3, 2009, pp. 245-250.

[8]. M. Zhan, Magnetic fluid and nanoparticle applications to nanotechnology, *Journal of Nanoparticle Research,* 3, 2001, pp. 73-78.

---